where $x(y)$ is the maximum value of x for a given y. The two parameters σ_τ and $\sigma_{\tau'}$ are then related by the relation

$$\sigma_{\tau'}-(3/m_\pi m_K)(g_{K\pi\pi\pi}/a_{\tau'})=-2\sigma_\tau. \quad (23)$$

The value of the parameter $a_{\tau'}$ is fixed by the τ' decay rate[17] to be

$$a_{\tau'}=[64(2\pi)^2 3^{3/2} m_K(\Gamma(\tau')/Q_{\tau'}{}^2)]^{1/2}=9.12\times10^{-7}.$$

Hence, we obtain the relation (in the unit of $m_\pi{}^{-2}$)

$$\sigma_{\tau'}=-2\sigma_\tau\pm0.13, \quad (24)$$

where the $\pm$ signs allow for the two possible relative phases of the two channels. The latest experimental information[15] consists of

$$\sigma_{\tau'}=(0.24\pm0.02)m_\pi{}^{-2}$$

and

$$\sigma_{\tau'}/\sigma_\tau=-2.3\pm0.4.$$

[17] G. Alexander, S. P. Almeida, and F. S. Crawford, Jr., Phys. Rev. Letters **9**, 68 (1962).

Although these data are not well correlated by our relation (24), the emergence of the ratio -2.3 is encouraging. As we have already remarked in the introduction, the value of the coupling constant $g_{K\pi\pi\pi}$ as given by (18) may be off by a factor of 2 or so. Within this limit, the relation (24) can indeed be consistent with the experimental result. Of course, more experimental effort to determine the σ parameters more accurately is desirable.

To make explicit the result already stated, we also record the relation

$$\sigma_{\tau'}=\sigma(+-0),$$

where $\sigma(+-0)$ refers to the energy spectrum of π^0 in the decay $K_2{}^0\to\pi^+{+}\pi^-{+}\pi^0$.

ACKNOWLEDGMENT

It is a pleasure to thank Professor Julian Schwinger for suggesting the problem and for subsequent advice and suggestions.

PHYSICAL REVIEW VOLUME 137, NUMBER 2B 25 JANUARY 1965

Strange-Particle Production by 3-BeV/c π^- Mesons in Hydrogen*

T. P. WANGLER, A. R. ERWIN, AND W. D. WALKER
Department of Physics, University of Wisconsin, Madison, Wisconsin
(Received 9 September 1964)

Over 600 strange-particle events were identified on the basis of both kinematical fitting and bubble-density information. The center-of-mass angular distributions generally show the familiar backward tendency for the baryons and forward tendency for the K mesons. Invariant mass distributions show the production of several resonant states including the $Y_1{}^*$(1385 MeV), K^*(885 MeV), and $Y_0{}^*$(1405 MeV). The two-body reactions $\pi^-+p\to K^*+Y_1{}^*$ and $\pi^-+p\to K^*+Y_0{}^*$ are also reported and studied. The two-, three-, and four-particle reactions are discussed and an attempt is made to put limits on the SU_3 multiplet of the f^0 from the number of $K_1{}^0K_1{}^0$ events with a mass near the f^0. The cross sections are calculated and the total strange-particle cross section at this energy is estimated to be $\sigma=(1.68\pm0.20)$ mb.

INTRODUCTION

FROM an analysis of 60 000 pictures of π^--p interactions at a pion momentum of 3 BeV/c in the B.N.L. 20-in. hydrogen bubble chamber, over 600 measured events were identified as strange-particle events. A complete scan of all the film was done for charged decays and neutral V's and two-thirds of the film was rescanned. The film was measured on digitized projectors and IBM-704 computer programs performed the tasks of geometrical reconstruction and kinematical fitting to the various mass hypotheses. A revised version of GUTS[1] formed the basis of the kinematical fitting program. Visual estimates of the bubble density of each track were also used in the analysis. All events found in the scanning were measured and analyzed except for single V events with zero prongs.

After the analysis was completed there were 437 events believed to be unambiguous fits to strange particle hypotheses, 130 events ambiguous between two categories, and 98 events with two or more neutral particles. Of the 130 ambiguous events 62 were ambiguous between $\pi^-K^+\Lambda^0$ and $\pi^-K^+\Sigma^0$. The remaining 68 events were distributed among the various categories according to the lowest χ^2. The χ^2 distributions for the one-constraint and four-constraint fits seen in Figs. 1(a) and 1(b), show good agreement with the theoretical distributions.

CROSS SECTIONS

The cross sections were determined by normalizing to the total cross section of 32.5 mb measured by a

* Work done under the auspices of the U. S. Atomic Energy Commission.
[1] J. P. Berge, F. T. Solmitz, H. D. Taft, Rev. Sci. Instr. **32**, 538 (1961).

counter experiment.[2] The number of observed interactions in the chamber was corrected for the unseen elastic events in the forward direction estimated from Ref. 3. Each event then corresponded to 0.88 μb.

To obtain each partial cross section the number of events observed for a given reaction was corrected for scanning efficiency, decays outside the chamber, decays in a distance too short to be seen, and for neutral decay modes of V's. The Σ^+ event cross sections were based upon the observed $\Sigma^+ \rightarrow \pi^+ + N$ events and were then corrected for the 50% proton decays.

Table I lists the number of events observed, the cross section, and cross-section error for the various reactions. The errors reported consist of the statistical error, a 10% error in the escape correction factor, and a 4% error in cross section per event, combined quadratically Those reactions involving $K_1^0K_2^0$ production generally were not studied in this experiment. Neglecting these events the total strange-particle cross section is

$$\sigma = 1.53 \pm 0.18 \text{ mb}.$$

If we assume that $\sigma(K_1^0K_2^0) = \sigma(K_1^0K_1^0) + \sigma(K_2^0K_2^0)$ and if we allow a 50% error for this number, an estimate of the total strange-particle cross section at this energy is

$$\sigma = 1.68 \pm 0.20 \text{ mb}.$$

Figure 2 shows the strange-particle cross section as a function of incident π^- momentum as estimated from different $\pi^- p$ experiments. Table II lists the number of observed events and estimated cross sections for reactions involving resonant states.

TABLE I. Cross sections.

Reaction	No.	σ (μb)	$\Delta\sigma$ (μb)	Reaction	No.	σ (μb)	$\Delta\sigma$ (μb)
$K^0\Lambda^0$	5	31	14	$K^-PK^0\pi^0$	9	32	11
$K^0\Sigma^0$	14	86	25	$K^+\pi^-K^0N$	2	7	5
$K^+\Sigma^-$	12	15	5	$\pi^+K^-K^0N$	5	18	8
$\pi^-K^+\Lambda^0/\Sigma^0$ [a]	80	136	21	$K^+K^-\pi^-P$	2	28	20
$\pi^0K^0\Lambda^0/\Sigma^0$	23	141	33	$\Sigma^+\pi^-K^0\pi^0$	9	41	17
$K_1^0K_1^0N$	19	52	13	$\Sigma^+\pi^-K^+\pi^-$	10	15	6
K^-PK^0	24	66	16	$\Sigma^-K^+\pi^+\pi^-$	24	29	7
K^+K^-N	4	56	29	$\Sigma^-\pi^+K^0\pi^0$	10	33	11
$\Sigma^+\pi^-K^0$	30	44	11	$\pi^-\pi^+\pi^0K^0\Lambda^0/\Sigma^0$	10	60	20
$\Sigma^-\pi^+K^0$	80	91	14	$\pi^-\pi^+\pi^-K^+\Lambda^0$	3	5	3
$\Sigma^-K^+\pi^0$	41	48	9	$\pi^-\pi^+K_1^0K_1^0N$	1	3	3
$K^+\Xi^-K^0$	1	1	1	$\pi^-PK_1^0K_1^0\pi^0$	1	3	3
$\pi^-\pi^+K^0\Lambda^0$	61	72	17	$\Sigma^+\pi^-\pi^+\pi^-K^0$	2	2	1
$\pi^-\pi^+K^0\Sigma^0$	26	86	19	$\Sigma^-K^+\pi^+\pi^-\pi^0$	4	5	3
$\pi^-\pi^0K^+\Lambda^0/\Sigma^0$	49	91	16	$\Sigma^-\pi^+\pi^+\pi^-K^0$	3	3	2
$K_1^0K_1^0N\pi^0$	6	17	7	$\pi^+\pi^-\pi^+\pi^-K^0\Lambda^0$	1	1	1
$\pi^-PK_1^0K_1^0$	8	10	5	$\pi^0\pi^0K^0\Lambda^0/\Sigma^0$	18	110	28
$\pi^-PK_1^0K_2^0$	6	9	4				

[a] Λ^0/Σ^0 means Λ^0 or Σ^0.

[2] A. N. Diddens, E. W. Jenkens, T. F. Kycia and K. F. Riley, Phys. Rev. Letters **10**, 262 (1963).

[3] V. Hagopian, Doctoral dissertation, University of Pennsylvania 1963 (unpublished).

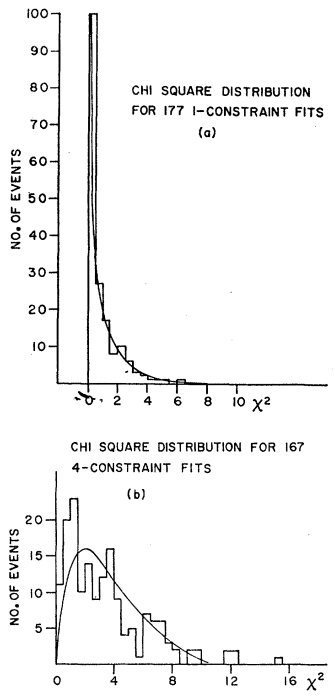

FIG. 1. χ^2 histogram (a) for 177 one-constraint fits from various reactions; (b) for 167 four-constraint fits from various reactions. The solid curves are the theoretical χ^2 distributions for one and four degrees of freedom, respectively.

FOUR-BODY HYPERON REACTIONS

Effective Masses from Λ^0 Reactions

Figure 3 shows the effective-mass plots for the reactions

$$\pi^- p \rightarrow \pi^-\pi^+K^0\Lambda^0 \quad 61 \text{ events} \qquad (1)$$

$$\rightarrow \pi^-K^+\Lambda^0\pi^0 \quad 43 \text{ events}. \qquad (2)$$

The solid curve shows the shape of the phase space

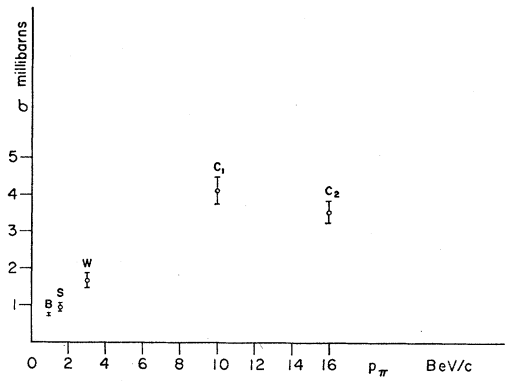

FIG. 2. Strange-particle cross section for $\pi^- p$ collisions versus incident-pion momentum in the laboratory as obtained from various experiments. The labels refer to the following sources: B—F. S. Crawford *et al.*, in *Proceedings of the International Conference on High Energy Physics at CERN* (CERN, Geneva, 1962), p. 271; S—J. Alitti *et al.*, in *The Aix-en-Provence International Conference on Elementary Particles, 1961* (Centre d'Études Nucléaires de Saclay, Seine et Oise, 1961), p. 375; W—data from this experiment; C_1—A. Bigi *et al.*, in *Proceedings of the International Conference on High Energy Physics at CERN* (CERN, Geneva, Switzerland, 1962), p. 247; C_2—J. Bartke *et al.*, Nuovo Cimento **24**, 876 (1962).

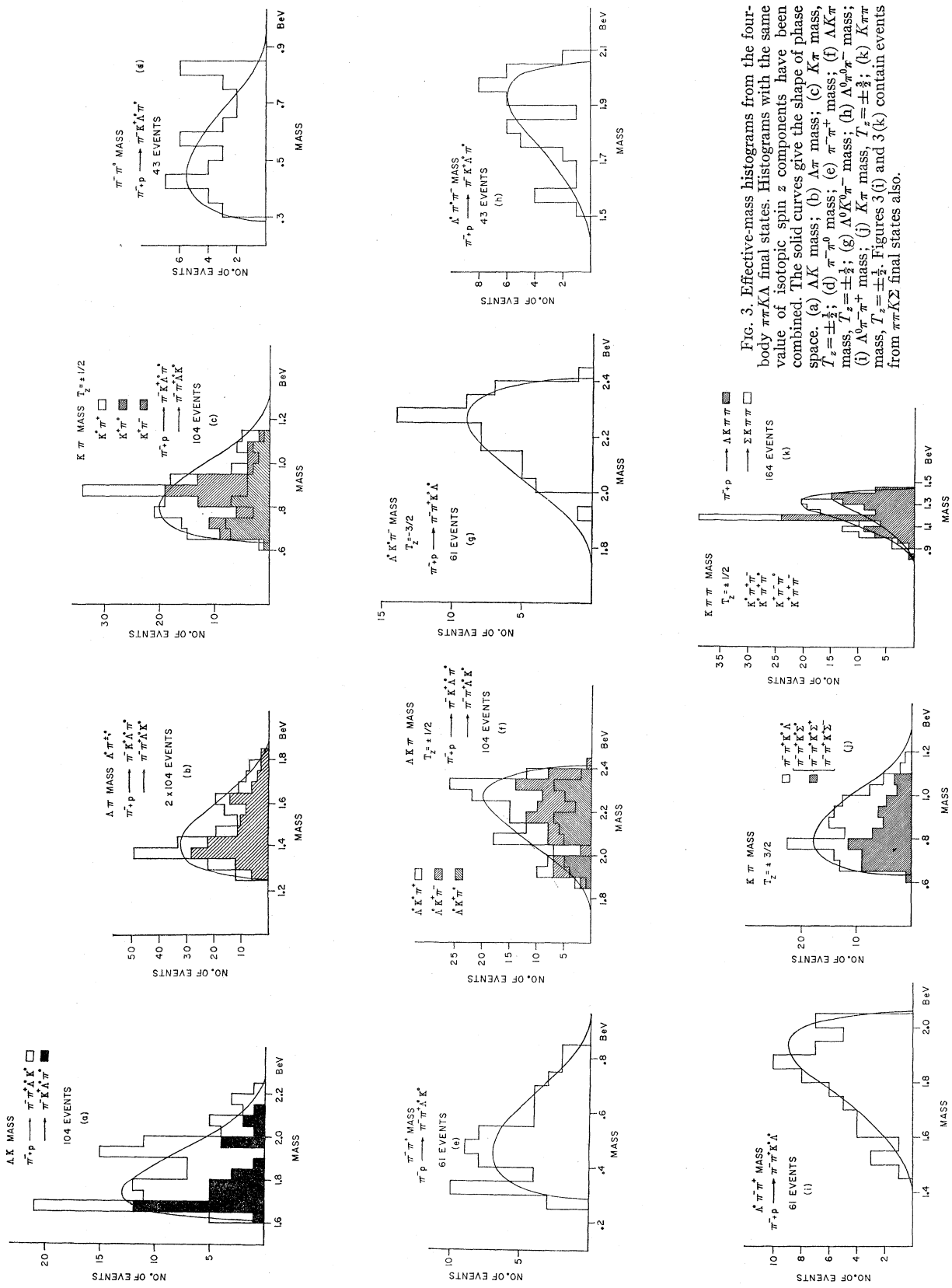

FIG. 3. Effective-mass histograms from the four-body $\pi\pi K\Lambda$ final states. Histograms with the same value of isotopic spin z components have been combined. The solid curves give the shape of phase space. (a) ΛK mass; (b) $\Lambda\pi$ mass; (c) $K\pi$ mass, $T_z=\pm\frac{1}{2}$; (d) $\pi^-\pi^0$ mass; (e) $\pi^-\pi^+$ mass; (f) $\Lambda K\pi$ mass, $T_z=\pm\frac{1}{2}$; (g) $\Lambda^0K^0\pi^-$ mass; (h) $\Lambda^0\pi^0\pi^-$ mass; (i) $\Lambda^0\pi^-\pi^+$ mass; (j) $K\pi$ mass, $T_z=\pm\frac{3}{2}$; (k) $K\pi\pi$ mass, $T_z=\pm\frac{1}{2}$. Figures 3(i) and 3(k) contain events from $\pi\pi K\Sigma$ final states also.

TABLE II. Special cross sections.

Reaction	No. Estimated	σ (μb)	$\Delta\sigma$ (μb)
$K^{*0}Y_0^*(1405)$	15	40	13
$K^+Y_1^{*-}(1385)$	6	11	5
$K^0Y_1^*(1385)$	3	18	11
$K^{*0}Y_1^{*0}(1385)$	11	30	13
$K^{*+}Y_1^{*-}(1385)$	<4	<10	
$K^0Y_0^*(1405)$	9	31	11
$K^0Y_0^*(1520)$	11	60	20
$K^{*0}\Lambda^0/\Sigma^{0}$ [a]	31	67	14
$\omega^0K^0\Lambda^0/\Sigma^0$	4	24	12
$N(f^0\to K\bar{K})$	8	88	33

[a] Λ^0/Σ^0 means Λ^0 or Σ^0.

distribution and is generally normalized to the total number of events. Reaction (2) may have a large contamination from $\pi^-p\to\pi^-K^+\Sigma^0\pi^0$ events.

The ΛK mass in Fig. 3(a) shows an almost significant peak in the vicinity of 1675 MeV. $I=\frac{1}{2}$ resonances have been reported in this region for πN total cross sections and for $\pi p\to\Lambda K$. The πN resonance appears to have high angular momentum, perhaps $f_{5/2}$, while the ΛK resonance seems to be $P_{1/2}$ or $P_{3/2}$.[4] Since $\pi p\to N\pi\pi\pi$ at our energy also shows only a weak effect at 1675 MeV,[5] it would appear that at most we are observing the $P_{1/2}$ or $P_{3/2}\Lambda K$ resonance in Fig. 3(a). Another indication of a bump appears near 1950 MeV, but there is no known resonance in this region with $T=\frac{1}{2}$.

The $\Lambda\pi$ mass in Fig. 3(b) shows the $Y_1^*(1385$ MeV).[4] A Gaussian ideogram of these events gives the Y_1^* at 1385 MeV with a full width $\Gamma=40$ MeV. The $K\pi$ mass for $T_z=\pm\frac{1}{2}$ in Fig. 3(c) shows the $K^*(885$ MeV). A Gaussian ideogram of these events gives the K^* at 895 MeV with a full width $\Gamma=40$ MeV. The distributions in Figs. 3(d) through 3(i) appear to show no significant deviations from phase space. Figure 3(j) is the $K\pi$ mass for $T_z=\pm\frac{3}{2}$ where we have combined the $\pi\pi K\Lambda$ events with the $\pi\pi K\Sigma$ events. The data do not seem to deviate significantly from the phase space distribution. The $K\pi\pi$ effective mass distribution contains a peak at 1175 MeV with a width of about 40 MeV. This plot, which is shown here in Fig. 3(k), has been discussed in a previous paper.[6]

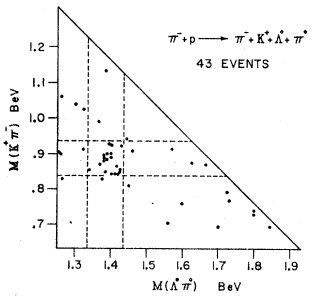

FIG. 4. Plot of the $K^+\pi^-$ effective mass against the $\Lambda^0\pi^0$ effective mass from 43 events fit $\pi^-K^+\Lambda^0\pi^0$. The kinematic limits are given by the sides of the triangle and the dashed lines define bands of width 2Γ centered on the known Y_1^* (1385-MeV) and K^* (885-MeV) resonances. $\Gamma=50$ MeV is taken for the width of each resonance.

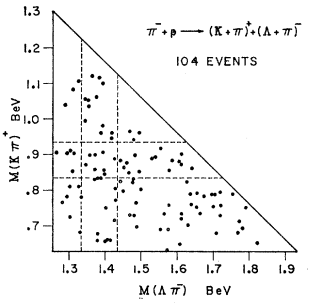

FIG. 5. Plot of $(K\pi)^+$ effective mass against the $(\Lambda\pi)^-$ effective mass for 104 events from the two $\Lambda K\pi\pi$ final states. The sides of the triangle give the kinematic limits and the dashed lines define the bands associated with the Y_1^* (1385-MeV) and K^* (885-MeV) resonances.

Two Body K^*-Y^* Production

Figure 4 shows 43 events from reaction (2) where the $\Lambda^0\pi^0$ mass is plotted versus the $K^+\pi^-$ mass. The triangular kinematic limits and the $Y_1^*(1385$ MeV) band and $K^*(885$ MeV) band are indicated. Nineteen events fall into the $K^*Y_1^*$ region where one expects only three events from a phase space distribution of 43 events. The strong correlation of K^* production with Y_1^* production is evident.

Figure 5 shows the plot of the $(\Lambda\pi)^-$ mass versus the $(K\pi)^+$ mass. The 104 events come from both reactions (1) and (2). For 104 events following a phase space distribution, seven events are expected in the region of the crossing bands and eight events are observed. The 19 $K^{*0}Y_1^{*0}$ events previously discussed are also present in Fig. 5 and upon examination are found to be smoothly distributed over the plot, none of them being in the region of the crossed bands. After removal of these 19 events one observes eight events in the $K^*Y_1^*$ region and six are expected.

The presence of $K^{*0}Y_1^{*0}$ and the absence of $K^{*+}Y_1^{*-}$ can be explained by the assumption of single-meson exchange. $K^{*0}Y_1^{*0}$ production could result from exchange of a K^+ or K^{*+} but $K^{*+}Y_1^{*-}$ production could occur only if the proton emitted a doubly charged positive meson and no such particle of low mass has been found. The forward tendency in the distribution of K^{*0} from $K^{*0}Y_1^{*0}$ events in the π^-p center of mass (Fig. 6) adds some support to this explanation. Using

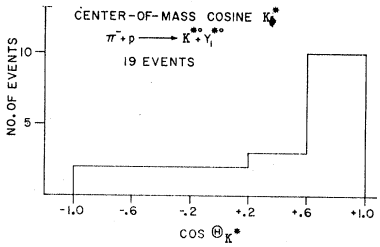

FIG. 6. Center-of-mass cosine between the outgoing K^* and the incident π^- for the 19 $K^{*0}Y_1^{*0}$ events.

[4] See Matts Roos, Rev. Mod. Phys. **35**, 314 (1963) for detailed references on resonant states.

[5] V. Hagopian (private communication).

[6] T. P. Wangler, A. R. Erwin, and W. D. Walker, Phys. Letters **9**, 71 (1964).

the procedure of Smith *et al.*[7] for the 19 $K^{*0}Y_1^{*0}$ events we find that a K to K^* exchange cross-section ratio of 0.43 ± 0.43 will explain the K^* decay angular distributions observed.

Λ^0 Polarization

The Λ^0 polarization was determined for the 19 $K^{*0}Y_1^{*0}$ events. The Λ^0 decay angular distribution is[8]

$$d\sigma/d\cos\theta = 1+\alpha\bar{p}_\Lambda\cos\theta,$$

where θ is the angle between the decay π and the production normal ($\pi_{\text{inc}}^-\times Y_1^*$) as viewed in the Λ rest frame,[9] $\bar{p}_\Lambda$ is the mean Λ^0 polarization, and $\alpha=-0.62\pm0.07$. Using the formula

$$\alpha\bar{p}=3(\sum_{i=1}^{N}\cos\theta_i)/N$$

with the error calculated from $\Delta(\alpha\bar{p}_\Lambda)=(3/N)^{1/2}$, we obtain for the polarization of the Λ^0, $\bar{p}_\Lambda=-0.95\pm0.65$.

Although the error is quite large for the Λ polarization the result is an indication that the sign of the Λ^0 polarization and hence that of the Y_1^{*0} is negative, i.e. opposite the direction ($\pi_{\text{inc}}^-\times Y_1^*$).

The Y_1^{*+}(1385 MeV) appears to be present in reaction (1),[10] and the polarization of Λ^0's from these events was investigated in the same way as for the

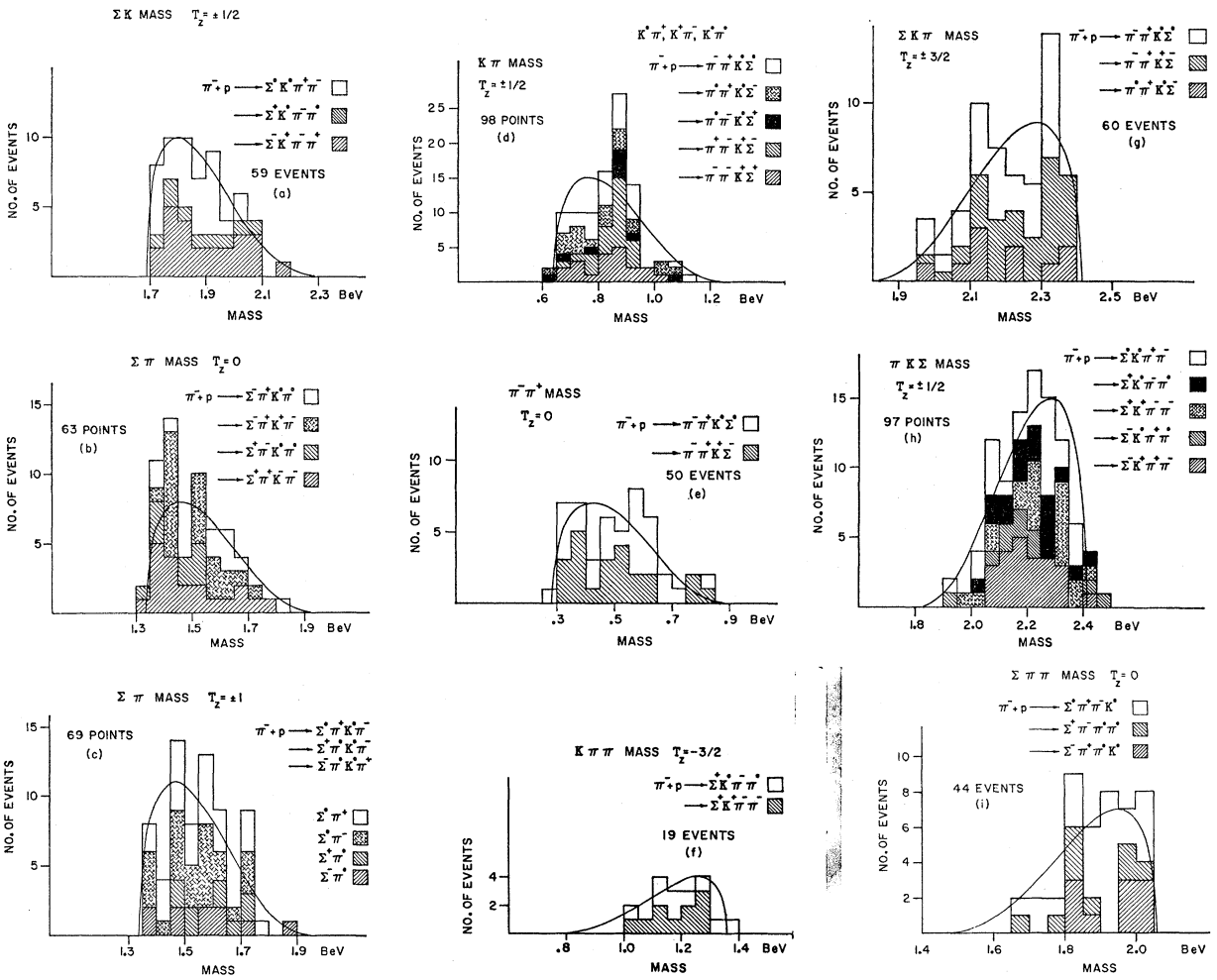

FIG. 7. Effective-mass histograms from the four-body $\pi\pi K\Sigma$ final states. Histograms with the same value of isotopic spin z component have been combined. The solid curves give the shape of phase space. (a) ΣK mass, $T_z=\pm\frac{1}{2}$; (b) $\Sigma\pi$ mass, $T_z=0$; (c) $\Sigma\pi$ mass, $T_z=\pm1$; (d) $K\pi$ mass, $T_z=\pm\frac{1}{2}$; (e) $\pi^-\pi^+$ mass, $T_z=0$; (f) $K\pi\pi$ mass, $T_z=-\frac{3}{2}$; (g) $\Sigma K\pi$ mass, $T_z=\pm\frac{3}{2}$; (h) $\pi K\Sigma$ mass, $T_z=\pm\frac{1}{2}$; (i) $\Sigma\pi\pi$, $T_z=0$.

[7] G. A. Smith, J. Schwartz, D. H. Miller, G. Kalbfleisch, R. W. Huff *et al.*, Phys. Rev. Letters **10**, 138 (1963).
[8] J. W. Cronin and O. E. Overseth, Phys. Rev. **129**, 1795 (1963).
[9] Chou Kuang-Chao and M. I. Shirokov, Zh. Eksperim. i Teor. Fiz. **34**, 1230 (1958) [English transl.: Soviet Phys.—JETP **7**, 851 (1958)].
[10] The Y_1^* events (1335 to 1435 MeV) seen in Fig. 3(b) which are associated with the reaction $\pi^-p\to\pi^-\pi^+\Lambda^0K^0$ are primarily due to $\Lambda^0\pi^+$ combinations.

Y_1^{*0} events from reaction (2). The Λ^0 polarization along the direction $(\pi_{\text{inc}}^- \times Y_1^*)$ is $\bar{p}_\Lambda = +1.09 \pm 0.60$ based upon 22 events. It is to be noticed that although the errors are large, the sign of the Λ° polarization along the direction defined appears to differ for Y_1^* production in reactions (1) and (2).

Effective Masses from Σ Reactions

Figure 7 shows the effective mass plots for the following reactions:

$$\pi^- p \rightarrow \pi^+\pi^- K^0\Sigma^0 \quad 26 \text{ events} \quad (3)$$

$$\rightarrow \Sigma^+\pi^- K^0\pi^0 \quad 9 \text{ events} \quad (4)$$

$$\rightarrow \Sigma^+ K^+\pi^-\pi^- \quad 10 \text{ events} \quad (5)$$

$$\rightarrow K^+\Sigma^-\pi^+\pi^- \quad 24 \text{ events} \quad (6)$$

$$\rightarrow \pi^+\Sigma^+ K^0\pi^0 \quad 10 \text{ events}. \quad (7)$$

The phase space distributions are given by the solid curves. Most of these plots are statistically consistent with their phase space distributions. However, the $K\pi$ system [Fig. 7(d)] shows the K^*(885 MeV), and the $\Sigma\pi$ system [Fig. 7(b)] shows a probable 1405 MeV Y_0^*.[4]

In Fig. 8 the $(\Sigma\pi)^0$ mass is plotted versus the $(K\pi)^0$ mass for the events from reactions (4) through (7). The K^*(885 MeV) and Y_0^*(1405 MeV) bands are shown. Although $K^* Y_0^*$ double resonant production seems to occur, there is no clearly significant trend for K^* production to be correlated with Y_0^* production, which is in contrast to the $K^{*0} Y_1^{*0}$ reaction (Fig. 4).

Angular Distributions

The angular distributions (not shown) for all seven 4-body hyperon reactions show a slight excess of hyperons in the backward direction (opposite the direction of the incident π^-) and a slight excess of K^0's in the forward direction, whereas the π's show no forward or backward preference.

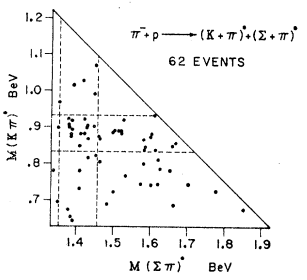

FIG. 8. Plot of the $(K\pi)^0$ effective mass against the $(\Sigma\pi)^0$ effective mass for 62 events from the $\pi\pi K\Sigma$ final states. The kinematic limits are given by the sides of the triangle and the dashed lines define bands of width 2Γ centered on the known Y_0^* (1405 MeV) and K^* (885-MeV) resonances. $\Gamma = 50$ MeV is taken for the width of each resonance.

THREE-BODY HYPERON REACTIONS

Effective Masses from Λ Production

The three-body reactions,

$$\pi^- p \rightarrow \pi^- K^+\Lambda^0 \text{ or } \Sigma^0 \quad 80 \text{ events} \quad (8)$$

$$\rightarrow \pi^0 K^0\Lambda^0 \text{ or } \Sigma^0 \quad 17 \text{ events}, \quad (9)$$

pose a problem because most of the events were ambiguous between Λ^0 and Σ^0 hypotheses. Figure 9 shows the mass plots for these reactions based upon the Λ^0 fits, except for 17 unambiguous cases of $\pi^- p \rightarrow \pi^- K^+\Sigma^0$. Figure 9(a) shows that Y_1^*(1385 MeV) production may not be very strong at this energy for the three-body Λ^0 reaction. The presence of the K^* is obvious in Fig. 9(b). A $K\pi$ mass distribution (not shown) based upon the Σ^0 fits and including the 17 unambiguous $\pi^- K^+\Sigma^0$ events agrees qualitatively with Fig. 9(b). About 40% of the events have their $K\pi$ mass between 835 and 935 MeV. The ΛK system in Fig. 9(c) shows no large peaks.

With the strong K^* production observed it is possible to make an analysis of the K^* decay angular distribution to determine the amount of K and K^* exchange required, assuming that these are the only production mechanisms.

Using the precedure of Smith *et al.*[7] for the 35 events from reaction (8) with $K\pi$ mass between 835 MeV and 935 MeV, we find that a K to K^* exchange cross-section ratio of 0.49 ± 0.25 will explain the K^* decay angular distribution observed. Although the error is large and although our sample includes both $\pi^- p \rightarrow K^*\Lambda^0$ and

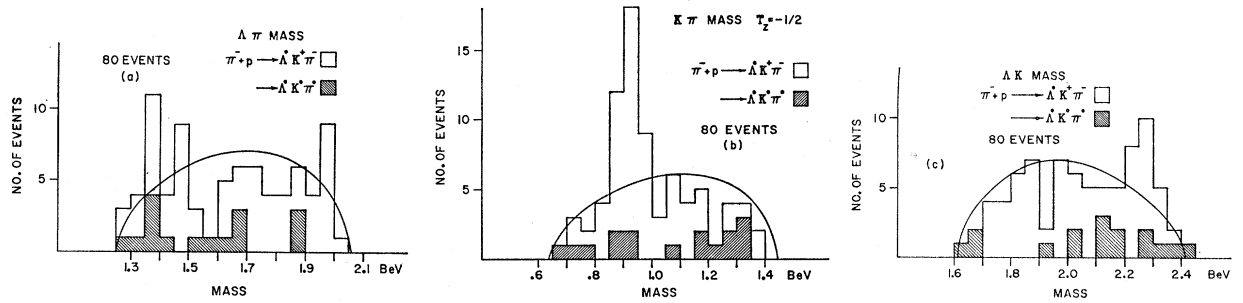

FIG. 9. Effective-mass histograms from 80 events which fit the two $\Lambda K\pi$ reactions. These histograms include both unambiguous $\pi^- K^+\Lambda^0$ events and events ambiguous between $\pi^- K^+\Lambda^0$ and $\pi^- K^+\Sigma^0$, but exclude 17 unambiguous $\pi^- K^+\Sigma^0$ events. (a) $\Lambda\pi$ mass; (b) $K\pi$ mass; (c) ΛK mass. The solid curves give the shape of phase space.

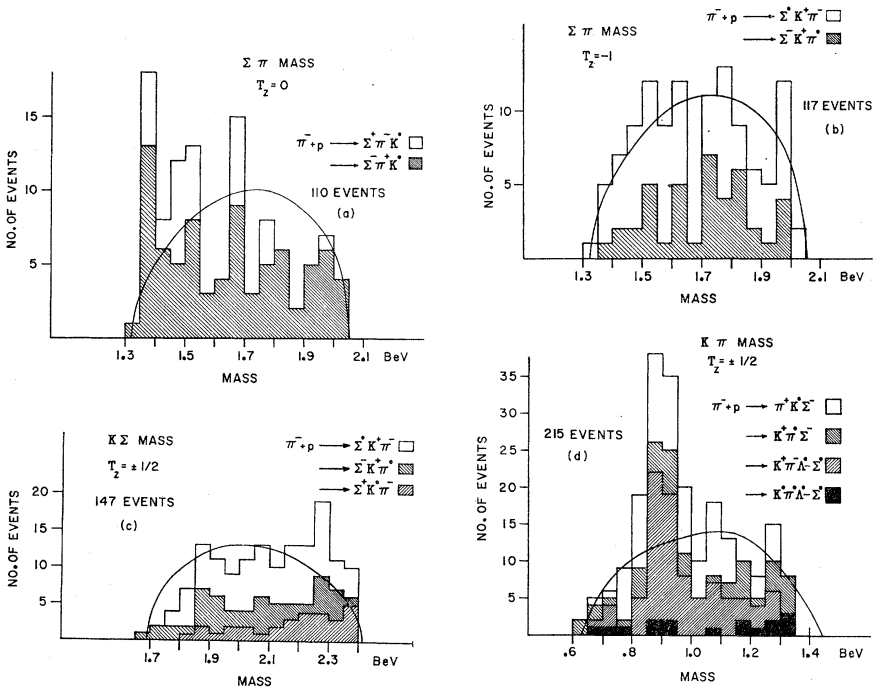

FIG. 10. Effective-mass histograms from the three-body $\Sigma K\pi$ final states. Histograms with the same value of isotopic spin z component have been combined. The solid curves give the shape of phase space. (a) $\Sigma\pi$ mass, $T_z=0$; (b) $\Sigma\pi$ mass, $T_z=-1$; (c) $K\Sigma$ mass, $T_z=\pm\frac{1}{2}$; (d) $K\pi$ mass, $T_z=\pm\frac{1}{2}$. Included in Fig. 10(d) are the ambiguous and unambiguous $\Sigma K\pi$ events from reactions (8) and (9).

$\pi^-p\rightarrow K^*\Sigma^0$, the result is nearly the same as those obtained in the reactions $\pi^-+p\rightarrow\Sigma^0+K^*$ at 2.17 and 2.25 BeV/c[7] and $\pi^++p\rightarrow\Sigma^++K^{*+}$ at 2.77 BeV/c.[11]

Effective Masses from Σ Production

Figure 10 gives the effective-mass plots for the $\Sigma K\pi$ reactions

$$\pi^-p\rightarrow\Sigma^+\pi^-K^0 \quad 30 \text{ events} \quad (10)$$
$$\rightarrow\Sigma^-\pi^+K^0 \quad 80 \text{ events} \quad (11)$$
$$\rightarrow\Sigma^-\pi^0K^+ \quad 41 \text{ events} \quad (12)$$
$$\rightarrow\pi^-K^+\Sigma^0 \text{ or } \Lambda^0 \quad 80 \text{ events}, \quad (8)$$

where the results of the Σ^0 fit are used for those events of reaction (8) which are ambiguous between the Λ^0 and Σ^0 hypotheses. The $\Sigma\pi$ mass for $T_z=0$ [Fig. 10(a)] shows what appears to be the 1405-MeV Y_0^*, and a bump at $\approx$1675 which, if it is real, could be either a 1680-MeV Y^* or a 1660-MeV Y^*.[4] There is, however, no indication of the 1660-MeV state in any other reaction. The $\Sigma\pi$ system for $T_z=-1$ [Fig. 10(b)] shows no known resonances. The ΣK system for $T_z=\pm\frac{1}{2}$ [Fig. 10(c)] has a small bump near 2275 MeV. It is interesting that this effect appears, although not significantly, in other reactions [see Figs. 3(f), 3(g), 7(g)] and might possibly be identified with the 2360-MeV pi-nucleon resonance listed in Ref. 4. Figure 10(d) seems to indicate that the $K\pi$ mass for $T_z=\pm\frac{1}{2}$ from reactions (8) through (12) is dominated by the K^*. However, only reaction (8) has a significant K^*.

Angular Distributions

The center-of-mass angular distributions in reactions (8) and (9), not shown, exhibit a tendency for forward

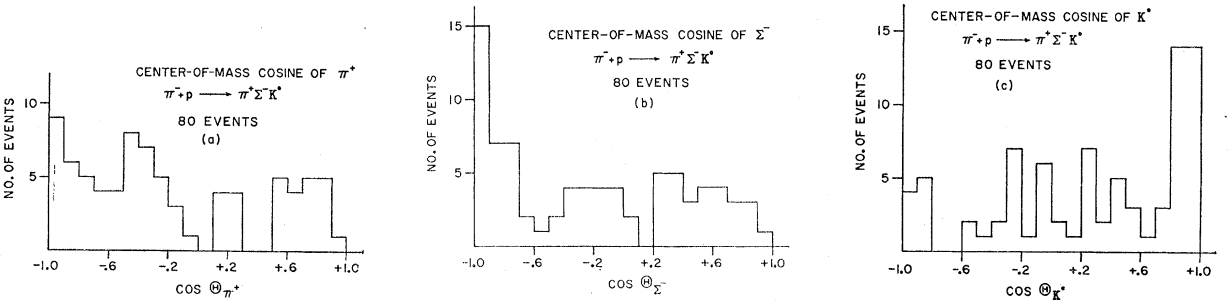

FIG. 11. Center-of-mass cosine of the angle with respect to the incident π^- for (a) π^+ (b) Σ^- (c) K^0 from the final state $\pi^+\Sigma^-K^0$.

[11] S. S. Yamamoto, L. Bertanza, G. C. Moneti, D. C. Rahm, and I. O. Skillicorn (to be published).

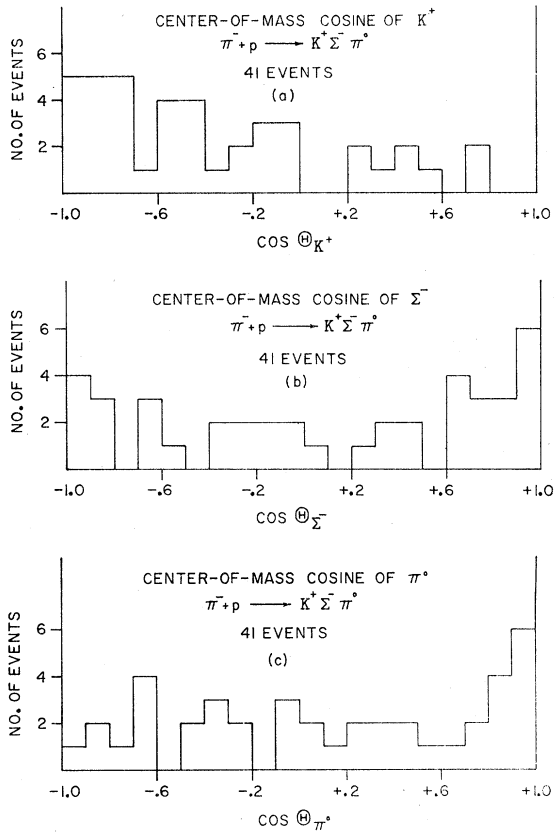

FIG. 12. Center-of-mass cosine of the angle with respect to the incident π^- for (a) K^+ (b) Σ^- (c) π^0 from the final state $K^+\Sigma^-\pi^0$.

π's and K's and backward hyperons. The hyperons present in the data are both Σ^0's and Λ^0's.

Figures 11 and 12 show the center-of-mass angular distributions from reactions (11) and (12). K^0's go predominantly forward and Σ^-'s go backward with respect to the incident beam direction in reaction (11). In contrast reaction (12) in which no resonant states appear to be dominant has a tendency for backward K^+'s and forward Σ^-'s. It is to be noticed that this is even more pronounced for the two-body production of $K^+\Sigma^-$. The angular distributions for reaction (10) are similar to those in reaction (11).

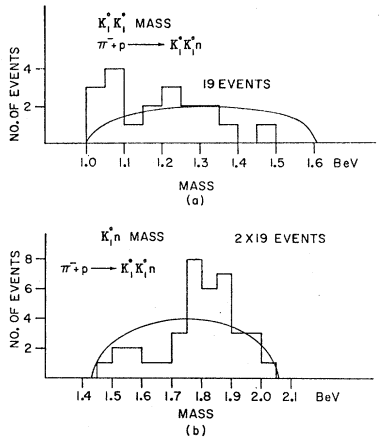

FIG. 13. Effective-mass histograms from the final state $K_1^0K_1^0N$. The solid curves give the shape of phase space. (a) $K_1^0K_1^0$ mass (b) K_1^0N mass.

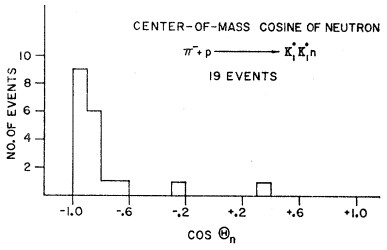

FIG. 14. Center-of-mass cosine of neutron with respect to the incident π^- for the 19 events from the final state $K_1^0K_1^0N$.

K-PAIR PRODUCTION

The statistical significance of all the K pair reactions is small. Still the results of

$$\pi^- p \rightarrow K_1^0K_1^0N \quad 19 \text{ events} \qquad (13)$$

$$\rightarrow K^-PK^0 \quad 24 \text{ events} \qquad (14)$$

are of interest. Figure 13 shows the $K_1^0K_1^0$ and K_1^0N effective masses from reaction (13). The $K_1^0K_1^0$ effective-mass distribution suggests the presence of the $K_1^0K_1^0$ s-wave enhancement at $\approx$1020 MeV previously seen in other experiments.[4] This same low $K_1^0K_1^0$ mass was also found all six $K_1^0K_1^0N\pi^0$ events observed. The center-of-mass angular distribution in Fig. 14 indicates a strong backward peaking of the neutron.

Figure 15 contains the effective masses from K^-PK^0 events. The K^-P system in Fig. 15(a) indicates the

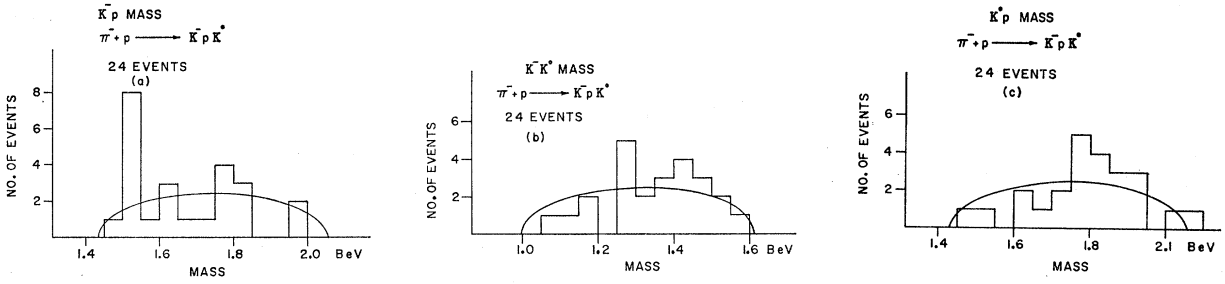

FIG. 15. Effective-mass histograms from the final state K^-PK^0. The solid curves give the shape of phase space. (a) K^-P mass (b) K^-K^0 mass (c) K^0P mass.

possibility of a strong $Y_0^*(1520\text{ MeV})$. The center-of-mass angular distributions from reaction (14) show a tendency for backward protons, but there is no sharp peaking as in reaction (13).

The $K_1^0K_1^0$ effective-mass distribution is of special interest since the $f^0(1250\text{ MeV})$[4] should decay into $K_1^0K_1^0$ if it has $I=0$, $J=2$ as reported by Lee *et al.*[12] An upper limit for the decay rate $f^0\rightarrow K_1^0K_1^0$ is obtained if we assume that all events with $K_1^0K_1^0$ effective mass[13] within ± 75 MeV of 1250 MeV result from f^0 decay. Correcting for $K_2^0K_2^0$ and K^+K^- events and using the data on $f^0\rightarrow\pi\pi$ at this energy,[3] we obtain

$$\sigma(f^0\rightarrow K\bar{K})/\sigma(f^0\rightarrow\pi\pi)=(16\pm 7)\%$$

as an upper limit to the branching ratio.

SU_3 predicts the branching ratio if the SU_3 multiplet to which the f^0 belongs is known.[14] The centrifugal barrier and phase space factors caused by the mass difference between the π and K will lower the ratio of $K\bar{K}/\pi\pi$ predicted by SU_3. The barrier factor was estimated assuming $J=2$ and an interaction radius in the range 0.5–0.7F. Table III lists the value of the branching ratios for the different possible f^0 representations in SU_3. In column 1 strict unitary symmetry is assumed and in columns 2 and 3 the number in column 1 is corrected for the barrier factor, assuming interaction radii of $\frac{1}{2}\hbar/m_\pi c$ and $\frac{3}{8}\hbar/m_\pi c$, respectively. The conclusion is that both the singlet and eightfold-symmetric assignments for the f^0 give predictions for the branching ratio which are consistent with the observed results.[15]

TABLE III. $(\bar{K}K)/(\pi\pi)$ Branching ratios for f^0 decay.

f^0 Representation	ratio from SU_3	Ratio with barrier of radius $\frac{1}{2}\hbar/m_\pi c$	Ratio with barrier of radius $\frac{3}{8}\hbar/m_\pi c$
1	4/3	0.33	0.23
8 symmetric	1/3	0.08	0.06
8 antisymmetric	∞	∞	∞
10	not allowed for $I=0$, $Y=0$	...	...
27	12	3.0	2.1

TWO-BODY PRODUCTION

The center-of-mass angular distributions (not shown) with respect to the incident π^- from the reactions

$$\pi^-p\rightarrow K^+\Sigma^- \quad 12\text{ events} \tag{15}$$

$$\rightarrow K^0\Lambda^0 \quad 5\text{ events} \tag{16}$$

$$\rightarrow K^0\Sigma^0 \quad 13\text{ events} \tag{17}$$

show a sharp forward peaking of the Σ^- in reaction (15) and a sharp forward peaking of the K^0 in reactions (16) and (17).

ACKNOWLEDGMENTS

We wish to thank the Shutt Bubble Chamber group at Brookhaven for providing us with the exposure in the 20-in. chamber, and Dr. Selove, Dr. Brody, and Dr. Hagopian from the University of Pennsylvania for cooperation in sharing the film. We also appreciate the help of Al Rhomberg and Bill Franks in handling the data, and the help of Dr. C. J. Goebel and Dr. Bunji Sakita in the interpretation of various aspects of the data.

[12] Y. Y. Lee, B. P. Roe, Daniel Sinclair, and J. C. Vander Velde, Phys. Rev. Letters **12**, 342 (1964).

[13] The width assumed ($\Gamma=75$ MeV) is consistent with that found for the f^0 from $\pi^-\pi^+N$ events in this experiment of $\Gamma=70\pm 20$ MeV (see Ref. 3).

[14] J. J. de Swart, Rev. Mod. Phys. **35**, 916 (1963).

[15] $K\bar{K}$ effective mass distrivutions with greater statistical significance have been reported by S. U. Chung, O. I. Dahl, L. M. Hardy, R. I. Hess, G. R. Kalbfleisch *et al.*, Phys. Rev. Letters **12**, 621 (1964), in an experiment with 3.22-BeV/c π^- in hydrogen. An enhancement at around 1310 MeV observed in both K^-K^0 and $K_0^1K_1^0$ is difficult to identify with the f^0. This result seems to suggest that greater statistics at our nearby energy would reveal a much smaller decay rate for f^0 into $K_1^0K_1^0$ than our upper limit.